Chemical Research in Toxicology®



Article

# Metabolic Activation and Cytotoxicity of Aloe-Emodin Mediated by Sulfotransferases

Ruihong Li, Wei Li, Yutong You, Xiucai Guo, Ying Peng, and Jiang Zheng

*Chem. Res. Toxicol.*, **Just Accepted Manuscript** • DOI: 10.1021/acs.chemrestox.9b00081 • Publication Date (Web): 03 May 2019



ACS Publications

is published by the American Chemical Society. 1155 Sixteenth Street N.W., Washington, DC 20036

# Metabolic Activation and Cytotoxicity of Aloe-Emodin Mediated by Sulfotransferases

Ruihong Li,† Wei Li,† Yutong You,† Xiucai Guo,† Ying Peng,*,† and Jiang Zheng*,†,§

†Wuya College of Innovation, Shenyang Pharmaceutical University, Shenyang, Liaoning, 110016, P.R. China
§State Key Laboratory of Functions and Applications of Medicinal Plants, Key Laboratory of Pharmaceutics of Guizhou Province, Guizhou Medical University, Guiyang, Guizhou, 550025, P.R. China

**Corresponding Authors:**

Jiang Zheng, PhD
Wuya College of Innovation, Shenyang Pharmaceutical University, No. 103, Wenhua Road, Shenyang, Liaoning, 110016, P. R. China
State Key Laboratory of Functions and Applications of Medicinal Plants, Key Laboratory of Pharmaceutics of Guizhou Province, Guizhou Medical University, 9 Beijing Road, Guiyang, Guizhou, 550025, P.R. China
Email: zhengneu@yahoo.com
Tel: +86-24-23986361; Fax: +86-24-23986510

†, §: The two corresponding units contributed equally to this work.

Ying Peng, PhD
Wuya College of Innovation, Shenyang Pharmaceutical University, No. 103, Wenhua Road, Shenyang, Liaoning, 110016, P. R. China
Email: yingpeng1999@163.com
Tel: +86-24-23986361; Fax: +86-24-23986510

## TOC Graphic

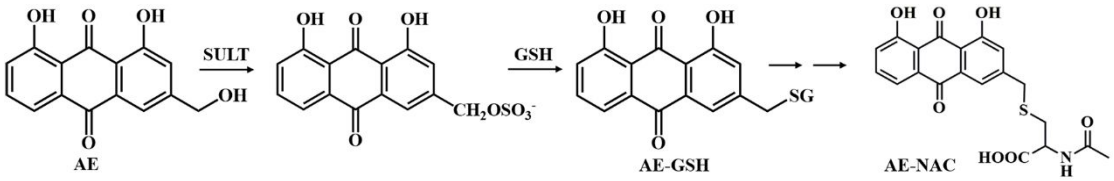
OH
O
OH
SULT
OH
AE
OH
O
OH
CH2OSO3-
GSH
OH
O
OH
SG
AE-GSH
OH
O
OH
S
HOOC
N
H
O
AE-NAC

**ABSTRACT**

Aloe-emodin (AE) is a major anthraquinone ingredient of numerous traditional Chinese medicines with a variety of beneficial biological activities *in vitro.* Previous studies suggested that AE possessed cytotoxicity and genotoxicity. Nevertheless, the mechanisms of the toxic action of AE have not yet been fully clarified. The present study aimed at characterization of metabolic pathways of AE to better understand the mechanisms of AE-induced cytotoxicity. An AE-derived glutathione conjugate (AE-GSH) was observed in rat liver cytosol incubations containing AE and GSH, along with 3′-phosphoadenosine-5′-phosphosulfate (PAPS). Similar incubation fortified with *N*-acetylcysteine (NAC) in place of GSH offered an AE-NAC conjugate corresponding to the GSH conjugate. The formation of the two conjugates was found to require PAPS. The two conjugates were respectively detected in bile and urine of rats given AE. Sulfotransferase (SULT) inhibitor pentachlorophenol (PCP) suppressed the production of the observed AE-GSH/NAC conjugates *in vivo*, suggesting that SULTs participated in the process of the metabolic activation of AE. The presence of PCP attenuated cell susceptibility to AE-induced cytotoxicity. The present study illustrated potential association of sulfation-mediated bioactivation of AE with its cytotoxicity.

## INTRODUCTION

Aloe-emodin (AE, 1, 8-dihydroxy-3-(hydroxymethyl)-anthraquinone), a natural polyphenolic anthraquinone, widely presents in Rhubarb (Rheum palmatum), Aloe vera and Senna and other traditional medicinal plants.[1-3] AE has shown extensive pharmacological effects including laxative, antifungal, antibacterial, antiviral and antimicrobial.[4-6] AE has a wide range of applications in clinic due to its high pharmaceutical values. It is reported that AE displayed anticancer activity against many kinds of cancerous cells, such as hepatoma, human lung carcinoma and leukemia cell lines, particularly for neuroectodermal tumor cells with high selectivity.[7-11] Given the planar chemical structure, a number of anthraquinones were found to intercalate into the structure of DNA especially at guanine or cytosine rich sites, which could result in DNA damage.[12-13] Furthermore, with a hydroxyl-methyl sidechain, AE was found to display mutagenicity in V79 cells, and DNA primary damage could be induced in rat hepatocytes using unscheduled DNA synthesis assay.[14] Previous study found that the cytotoxicity of AE might be attributed to their potent GSH depletion and DNA binding affinity.[15]

Sulfotransferases (SULTs), one of important phase II enzymes, play critical roles in metabolism of a great deal of endogenous and exogenous compounds, including neurotransmitters, thyroid, steroid hormones, therapeutic drugs and some chemical carcinogens.[16,17] The major role of SULTs is to catalyze transfer of a sulfonyl group to amino, hydroxyl, *N*-oxide or sulfhydryl group of the substrate molecules from 3′-phosphoadenosine-5′-phosphosulfate (PAPS).[18] Generally, relatively lipophilic

xenobiotics become more polar and easier to be excreted via sulfation. However, it has been proved that sulfation can activate some types of mutagens and chemical carcinogens.[19,20] The benzylic position of many drugs tend to be oxidized by P450 enzymes to form benzylic alcohol, and then sulfation can happen under the catalysis of SULTs. The highly reactive electrophilic species are formed because of the departure of the sulfonyl group, increasing the possibility of toxicity. Diao et al. found 3-OH-butylphthalide (NBP) could be metabolized to 3-OH-NBP sulfate via sulfation mediated mainly by SULT 1A1, and the resulting metabolite could be captured by GSH, proving its potential association with the hepatotoxicity of NBP.[21] Yuji Ishii et al. found the benzylic alcohol of lucidin could be metabolized to lucidin sulfate, which would react with DNA bases.[22]

Our earlier study demonstrated that AE either directly reacted with GSH due to its own electrophilic quinone moiety, or was metabolized to hydroxylated AE and the corresponding quinone mediated by P450 enzymes.[23] However, the effects of SULTs on the metabolism and the cytotoxicity of AE have not been covered. It would be important to verify whether this metabolic pathway is associated with cytotoxicity of AE. The objectives of the present work were to study the metabolic activation of AE *in vitro* and *in vivo* and explore the contribution of sulfation pathway to the development of AE cytotoxicity. We anticipated that this work would help us to understand the cytotoxicity of AE better.

## EXPERIMENTAL PROCEDURES

### Chemicals and materials.

AE with a purity of more than 98% was supplied by Dalian Meilun Biotech Co., Ltd. (Dalian, China). Glutathione (GSH) and *N*-acetylcysteine (NAC) were supplied by Aladdin Reagent Co., Ltd. (Shanghai, China). Propranolol, *S*-hexylglutathione and 3′-phosphoadenosine-5′-phosphosulfate (PAPS) were obtained from Sigma-Aldrich (St. Louis, MO). Pentachlorophenol (PCP) was supplied by Dr. Ehrenstorfer GmbH (Augsburg, Germany). Rat (Sprague-Dawley, male) liver cytosol (RLC) was prepared referring to a previously published method.[24] Distilled water was obtained from Wahaha Co., Ltd. (Hangzhou, China). All organic solvents were purchased from Fisher Scientific (Springfield, NJ). All of the reagents and solvents were analytical or high-performance liquid chromatography grade.

### Incubation of AE in rat liver cytosol.

The stock solution was prepared by dissolving AE in dimethyl sulfoxide (DMSO). The total proportion of the organic solvent in the incubation system was kept below 1%. The incubation mixture (100 μL) consisted of phosphate-buffered saline (PBS, 0.1 M, pH 7.4), $MgCl_2$ (3.2 mM), RLC protein (2.0 mg protein/mL), AE (100 μM) and trapping agents GSH/NAC (20 mM). PAPS (250 μM) was added to initiate the cytosol reactions. Negative control (without PAPS) was included to investigate the contribution of SULTs to the metabolic activation of AE. After 1 h incubation at 37 °C, 100 μL ice-cold acetonitrile (1:1 v/v) was added to quench the biochemical reaction, and the resulting mixture was vortexed for 30 s and centrifuged

for 10 min at 19,000 *g*. The resultant supernatants (10 μL) were injected to LC-MS/MS for analysis. All incubation reactions were performed in duplicate.

**Chemical synthesis of 3-(bromomethyl)-1, 8-dihydroxyanthracene-9, 10-dione (1).**

Synthesis of compound **1** (AE-Br) was achieved by bromination of AE (Scheme 1) as described by Shao et al.[25] In brief, phosphorus tribromide (950 μL, 10 mmol) was dropwise mixed with AE (540 mg, 2 mmol) dissolved in tetrachloromethane (35 mL). The resultant mixture was stirred at 65 °C for 3 h, and the reaction was monitored by TLC until completed. After cooling to ambient temperature, the resulting mixture was extracted by 30 mL dichloromethane twice. The combined organic layer was rinsed by 30 mL saturated $NaHCO_3$ aqueous and dehydrated by anhydrous sodium sulfate. Purification was performed by silica gel column chromatography. The product obtained was characterized by MS and NMR. $^1$H NMR (DMSO-$d_6$, 600 MHz): $\delta$ 4.82 (2H, s, -$CH_2$-), 7.40 (1H, d, Ar-H, $J$ = 8.34 Hz), 7.47 (2H, s, Ar-H), 7.73 (1H, d, Ar-H, $J$ = 7.26 Hz), 7.79 (1H, s, Ar-H), 7.82 (1H, dd, Ar-H, $J$ = 7.86, 7.92 Hz), 11.92 (2H, s, Ar-OH) (Figure S2).

**Synthesis of AE-GSH/NAC conjugates.**

GSH (276 mg, 0.9 mmol) or NAC (147 mg, 0.9 mmol) was dissolved in 3 mL DMSO, followed by mixing with 30 mg compound **1** (0.09 mmol). After 30 min stirring at room temperature, the reaction mixture was lyophilized and reconstituted with acetonitrile/water (50:50， v/v) for purification by a semi-preparative HPLC system. The purified products were characterized by MS and $^1$H NMR (Figure S3-4).

**Animal experiments.**

All animal experiments were carried out in accordance with the Animal Experimental Regulations of Ethics Review Committee of Shenyang Pharmaceutical University. Sprague-Dawley rats (220 ± 10 g, male) were supplied by the Animal Center of Shenyang Pharmaceutical University. Animals were fed with tap water and normal rat diet ad libitum and maintained at a dark/light period for 12 h in 25 °C. Six rats were randomly divided into two groups. The animals were fasted for 12 h and anesthetized by administration (i.p.) of chloral hydrate (10%) at a dose of 3.0 mL/kg. Bile ducts were cannulated, and first 30 min bile secreted was collected as blank. Successively, the animals were administered (i.p.) AE at a dose of 200 mg/kg dissolved in corn oil, and bile samples were collected for 12 h. The other three rats treated with the same dosage of AE were individually placed in metabolism cages. Urine samples were collected for 24 h, and the animals were allowed to access to food. Blank urine samples were collected from animals that had been fasted but free to drink water for an overnight before AE administration.

In a separate experiment, rats were pretreated (i.p.) with PCP dissolved in corn oil at a dose of 10 mg/kg.[26] One hour later, animals were administered with a single dose of AE (200 mg/kg, i.p.) or corn oil. Bile (0-12 h) and urine samples (0-24 h) were collected after administration.

**Sample preparation.**

The harvested bile samples (2 mL) were spiked with 50 μL of *S*-hexylglutathione (3.0 μg/mL) dissolved in acetonitrile, along with 6 mL ice-cold acetonitrile. The

resulting mixture was vortexed, centrifuged, concentrated by blowing with nitrogen gas, and analyzed by LC-MS/MS. Similar procedure was applied for urine sample preparation except for mixing with 50 μL propranolol (0.6 μg/mL) dissolved in acetonitrile in place of *S*-hexylglutathione as internal standard.

**Cytotoxicity evaluation.**

The cytotoxicity of AE was evaluated using MTT test.[27] HepG2 cells were seeded in a 96-wells plate with a density of $8\times10^3$ cells/well and allowed to adhere overnight. Cells were mixed with AE at concentrations of 0, 12 and 50μM. In a separate experiment, cells were mixed with SULT inhibitor PCP (6.25 μM). After 1 h incubated at 37 °C in a humidified incubator with 5% $CO_2$, the pretreated cells were mixed with AE at various concentrations. The AE-fortified cells of the two groups were incubated at 37°C for 48 h, followed by addition of 10 μL of MTT solution (5.0 mg/mL). The media were discarded 4 h later, and DMSO (100 μL) were added to dissolve the formazan crystals. Cell viability was determined by measuring the absorbance at 562 nm. The cytotoxicity tests were conducted in triplicate.

**LC-MS/MS methods.**

Sample analysis was performed on an AB SCIEX Instruments 5500 triple quadrupole mass spectrometer (Applied Biosystems, Foster City, CA) coupled to an Agilent 1260 infinity HPLC system with an autosampler (Agilent Technologies, Biblingen, Germany). The temperature of the turbo ion spray was set at 650 °C, and the entrance potential and ion spray voltage were 10 V and 5,500 V, respectively. The

mass spectrometric parameters were set as follows: declustering potential (50 V), curtain gas (20 psi), cell exit potential (3 V) and entrance potential (10 V). Chromatographic separation was carried out using an Accuore $C_{18}$ reverse column (4.6×150 mm, 5 μm; Thermo Fisher, Pittsburgh, PA). The analyte was eluted with a mobile system composed of solvent A (0.1% formic acid) and solvent B (acetonitrile containing 0.1% formic acid). Analyte separation was achieved by a linear gradient elution method: 0-2 min (10% B), 2-12 min (10 % to 90% B), 12-17 min (90% B), 17-18 min (90% to 10% B) and 18-20 min (10% B). The flow rate was set at 0.8 mL/min, and the column temperature was kept at 25 °C. Multiple-reaction monitoring (MRM) scanning, along with positive ion mode, was applied to achieve the optimal response for the analysis. Precursor/product ion pairs (declustering potential DP, collision energy CE) at *m*/*z* 271/225 (110, 35), *m*/*z* 560/253 (110, 35), *m*/*z* 416/253 (100, 35), *m*/*z* 392/246 (86, 24) and *m*/*z* 260/116 (77, 25) were selected for the analysis of AE, AE-GSH, AE-NAC, *S*-hexylglutathione, and propranolol, respectively.

Additionally, AB SCIEX Instruments 4000 Q-Trap (Applied Biosystems, Foster City, CA) coupled to an Agilent 1260 infinity HPLC system (Agilent Technologies, Biblingen, Germany) was also applied to analyze AE and its metabolites by means of enhanced product ion (EPI) scans in positive mode with a scan range from *m*/*z* 50 to 700 Da. EPI was triggered by the information-dependent acquisition (IDA) method. IDA was set to select ions more than 2000 cps with the exclusion of former target ions after three occurrences for 10 s and the EPI was for product ions. Collision energy (CE) was 32 ± 10 eV. All data obtained were analyzed by AB SCIEX Analyst 1.6.2

software (Applied Biosystems).

In addition, a hybrid quadrupole-time-of-flight mass spectrometer (Bruker micro Q-TOF, Germany) with an ESI source interfaced in-line with an Agilent 1200 Series LC system was employed in positive mode to characterize synthetic products. Related mass spectrometric parameters were set as follows: end plate offset = 2,500 V; capillary voltage = -4,500 V; dry gas flow rate = 8.0 L/min; nebulizer gas pressure = 1.2 bar. Temperature was maintained at 180 °C. Spectra were obtained at 2 s per spectrum from *m*/*z* 50 to 1,500. The same LC conditions were applied as mentioned above. Data were analyzed by Bruker Daltonics Data Analysis 3.4 software.

**Statistical analysis.**

All data were expressed as means ± SD. Unpaired Student's t-test was applied for statistical analysis. The values of $p < 0.05$ were deemed to have significant difference.

## RESULTS

### *In vitro* metabolic activation of AE.

GSH and NAC were employed to trap potential electrophilic species generated in RLC incubations. Noteworthy, an AE-derived GSH conjugate (AE-GSH) was detected in GSH-fortified RLC incubations, while incorporation of PAPS dramatically increased (approximately 10 fold) the generation of such conjugate (Figure 1A,B). As expected, the corresponding NAC conjugate (AE-NAC) was detected in NAC-supplemented RLC incubations. Such incubations spiked with PAPS offered 3-fold more AE-NAC conjugate than that of vehicle-spiked incubations (Figure 2A,B). This indicates that the formation of AE-GSH/NAC conjugates was PAPS-dependent and suggests that sulfation was involved in the formation of the electrophilic intermediate.

AE-GSH conjugate (RT=9.4 min) was detected by acquiring precursor/product ion pair at *m*/*z* 560/253 (Figure 1B). In order to further characterize the chemical structure of AE-GSH conjugate, tandem mass spectrometry (MS/MS) spectrum of AE-GSH was acquired in positive mode (Figure 1D). Ion of *m*/*z* 253, the major product ion, was produced by the break of the C-S bond of the conjugate. The neutral loss (NL) of the γ-glutamyl moiety (-129 Da) from *m*/*z* 560 led to the production of the characteristic fragment ion *m*/*z* 431. The formation of the product ions at *m*/*z* 485 and 414 from *m*/*z* 560 was due to the cleavage of the glycine group (-75 Da) and the glutaminyl group (-146 Da), respectively. The characteristic ion at *m/z* 311 from *m/z* 414 was generated by the break of the *N*-formylglycinyl group (-103 Da).

AE-NAC conjugate (RT=11.98 min) was detected by monitoring ion pair *m*/*z*

416/253 (Figure 2B). The characteristic fragment ion at *m*/*z* 285 of AE-NAC was acquired by MRM-EPI scanning, and the ion was produced by the break of the sulfur-carbon bond in NAC moiety (-129 Da) (Figure 2D). The primary product ion of *m*/*z* 253 was formed by the elimination of whole NAC portion, suggesting the presence of the aliphatic and/or benzylic thioether motif in the conjugate. The loss of acetyl group (-43 Da) resulted in the formation of product ions *m*/*z* 374, and ion *m*/*z* 130 arose from S-C cleavage at NAC side. Furthermore, the observed fragment ion *m*/*z* 225 was the most characteristic fragment for the parent moiety.

**Characterization of synthetic AE-GSH/NAC conjugates.**

Chemical synthesis was conducted to verify the structures of AE-GSH/NAC conjugates. AE sulfate is believed to be produced through the metabolism of AE mediated by SULTs. However, AE sulfate is chemically reactive and very unstable, and compound **1** (AE-Br) as an electrophilic synthon was synthesized in order to acquire AE-GSH/NAC conjugates.

Compound **1** (AE-Br) was synthesized by bromination of AE (Scheme 1) and analyzed by LC-MS/MS. As expected, compound **1** was detected (RT=13.6 min) by MRM scanning of *m*/*z* 333/254 and 335/254 in the reaction mixture (Figure 3). The mass spectrum showed a clear 1:1 ratio bromine isotope signals. Afterwards, compound **1** was mixed with GSH or NAC to offer AE-GSH/NAC conjugates. The protonated molecular ions of synthetic AE-GSH/NAC conjugates were *m/z* 560.1332 and *m/z* 416.0795 (Q-TOF), respectively. According to the prediction formula, the error between the accurate mass observed in the high-resolution MS system and the

corresponding theoretical mass was less than 5 ppm (Table 1).

The chromatographic and mass spectrometric properties of synthetic AE-GSH (Figure 1C,E) were consistent with that of AE-GSH conjugate formed in RLC incubations (Figure 1B,D). Similar observation was obtained regarding the chromatographic and mass spectrometric behaviors of synthetic AE-NAC conjugate (Figure 2C,E) and that generated in RLC incubations (Figure 2B,D). In addition, we succeeded in characterization of the two conjugates by $^{1}$H NMR (Figure 4B).

**Biliary and urinary metabolites of AE.**

Abundant excretions of biliary AE-GSH and urinary NAC-AE conjugates indicates the generation of reactive intermediates derived from AE *in vivo*. After intraperitoneally administration of AE in rats, bile samples were collected and injected to LC-MS/MS system for analysis. AE-GSH conjugate with protonated molecule at *m*/*z* 560 was detected in the bile of rats given AE, and no such metabolite was found in blank bile (Figure 5A,B). In addition, the conjugate exhibited consistent chromatographic and mass spectrometric behaviors as that formed in RLC incubations (Figure 1B,D and 5B,C). Similarly, urinary AE-NAC conjugate with protonated molecule at *m*/*z* 416 was detected in rats given AE, and no such metabolite was observed in blank urine (Figure 5D,E). The chromatographic and mass spectral properties of the urinary AE-NAC conjugate were consistent with that observed in RLC incubations (Figure 2B,D and 5E,F).

**Effect of PCP on formation of AE-GSH/NAC conjugates.**

PCP as a general inhibitor of SULTs was used to verify the role of SULTs in the formation of AE-GSH/NAC conjugates *in vivo*. Bile samples and urine samples were taken for 12 h or 24 h post injection of AE. The contents of biliary AE-GSH conjugate and urinary AE-NAC conjugate were assessed by LC-MS/MS. Rats pretreated with PCP displayed decreased excretion of biliary AE-GSH conjugate (79% decreased) and AE-NAC conjugates (73% decreased), compared with rats administrated AE alone ($p < 0.02$) (Figure 6).

**Cytotoxicity of AE in HepG2 cells.**

To define the relationship between cytotoxicity of AE and the sulfation pathway mediated by SULTs, cytotoxicity of AE was evaluated in HepG2 cells. Concentration-dependent toxicity was observed when cells were exposed to AE at various concentrations for 48 h. Pretreatment with PCP (a general SULT inhibitor) was found to attenuate AE-induced cytotoxicity (Figure 7).

## DISCUSSION

AE, one of the major active anthraquinone compounds in traditional medicinal plants, was widely used in China. The genotoxicity and cytotoxicity of AE were reported recently, and the mechanisms of the toxicities remain unknown. In the present work, we proposed a metabolic activation pathway of AE mediated by SULTs to help us understand the cytotoxicity of AE better.

Sulfotransferase is a cytosol enzyme responsible for sulfation metabolism pathway. RLC incubations were carried out to determine the involvement of sulfation in metabolic activation of AE. GSH and NAC were employed as trapping reagents. For soft electrophilic species, GSH is the most common trapping agent used *in vitro* incubations.[28] An AE-derived GSH conjugate was detected in AE-supplemented RLC incubations, and incorporation of PAPS dramatically enhanced the formation of the GSH conjugate (Figure 1A,B). This indicates that sulfation participated in the metabolic activation. It is not surprising that the GSH conjugate was detected in RLC incubations without spiking of PAPS, since the pre-prepared RLC contained some PAPS from liver tissues harvested. As expected, the corresponding AE-NAC conjugate was observed in AE- and NAC-supplemented RLC, and addition of PAPS in the incubations resulted in elevated formation of the NAC conjugate (Figure 2A,B). The *in vitro* NAC trapping work assisted us to characterize urinary AE-NAC conjugates. The observed AE-GSH/NAC conjugates *in vitro* were found to require PAPS, suggesting that the metabolic activation of AE was mediated by SULTs.

Chemical synthesis was conducted to facilitate metabolite identification. In

present study, bromination reaction was substituted for sulfation to generate a reactive carbocation. Compound **1** (AE-Br) was synthesized as an electrophilic synthon to take the advantage of the good leaving characteristic of bromide group. Purified compound **1** was characterized by LC-MS/MS analysis and NMR (Figure 3). The mass spectrum showed a distinctive 1:1 ratio bromine isotope peak (*m*/*z* 333/254 and *m*/*z* 335/254), and benzyl proton shift value was 4.82 ppm on NMR. This confirms that the bromination occurred at benzyl carbon atom. Afterwards, AE-GSH/NAC conjugates were obtained by the reaction of compound **1** with GSH/NAC in high yields. The two conjugates were characterized by LC-Q-TOF MS analysis and NMR. The results (Table 1) showed that the protonated molecular ion of AE-GSH/NAC conjugates matches the expected molecular formula ($C_{25}H_{25}N_3O_{10}S$/$C_{20}H_{17}NO_7S$) respectively, and the benzyl proton shift of the two synthetic conjugates were at 3.90 ppm and 3.72 ppm separately, which provided a solid evidence for the formation of AE-GSH/NAC conjugates (Figure 4).

Biliary GSH conjugates are commonly regarded as biomarkers of exposure to electrophilic species.[29] GSH conjugates are known to undergo hydrolytic cleavage of glutamic acid and glycine residues by $\gamma$-glutamyltranspeptidase and dipeptidases to form cysteine conjugates. Mercapturic acids (NAC conjugates) are finally produced through further *N*-acetylation.[30] As expected, biliary AE-GSH conjugate and urinary AE-NAC conjugate were observed in rats given AE (Figure 5 B,E). The two conjugates showed consistent mass spectral fragment patterns and retention time (Figure 5 B-F) with those of the corresponding metabolites detected in RLC incubations

(Figure 1 B,D and 2 B,D). Pretreatment with general SULT inhibitor PCP dramatically suppressed the excretion of AE-GSH/NAC conjugates (Figure 6), which indicates the involvement of SULTs in the metabolic activation of AE.

The association of AE-induced cytotoxicity with its bioactivation mediated by sulfation was investigated in HepG2 cells. AE revealed concentration-dependent cytotoxicity, and the addition of PCP markedly attenuated cell susceptibility to AE cytotoxicity (Figure 7), which suggests that the sulfation pathway played a certain role in AE-induced cytotoxicity.

Many drugs or their metabolites contain hydroxyl or amino groups attached to benzylic, allylic, or aromatic-allylic systems. These groups are metabolized to the corresponding sulfates catalyzed by SULTs. As a result, highly reactive electrophilic species are formed which are prone to attack nucleophilic cellular components. The modification may trigger varieties of toxicities. A putative metabolic activation pathway of AE is shown in Scheme 1. The benzyl hydroxyl of AE was not a reactive electrophile per se, however, it might undergo sulfation to produce AE sulfate, then further reacted with GSH/NAC by $S_N1$ or/and $S_N2$ reaction(s). The AE sulfate is chemically reactive, either generating a highly reactive electrophilic carbocation, which could react endogenous GSH to form AE-GSH conjugate ($S_N1$ mechanism), or/and being directly attacked by GSH ($S_N2$ mechanism). Both types of reactions would induce cellular GSH depletion.

Three types of GSH conjugates were detected in bile samples of rats given AE, including M3/M4, M6 and AE-GSH, and the first three were reported by our group[23].

These conjugates are derived from AE itself, quinone metabolites of AE, and AE sulfate. Apparently, more AE-GSH was produced than M3/M4 and M6 (Figure S5), although it was a semi-quantitative analysis. The roles of the three types of electrophilic specie in the development of AE toxicities need to be investigated.

In summary, we have characterized a new metabolic activation pathway of AE. Metabolism of AE undergoes sulfation, and the resulting AE-derived sulfate is chemically reactive to thiols. The phase II metabolism of AE may be a factor responsible for AE-induced cytotoxicity.

**Funding sources**

This work was supported in part by the National Natural Science Foundation of China [Grants 81430086, 81773813, 81830104].

**Notes**

The authors declare no competing financial interest.

**Supporting information**

Structure and MS/MS spectrum of AE; $^{1}$H NMR spectrum of compound **1** (AE-Br); The $^{1}$H NMR spectrum of AE-GSH conjugate; $^{1}$H NMR spectrum of AE-NAC conjugate; Biliary GSH conjugates derived from AE.

**Abbreviations**： CE, collision energy; DMSO, dimethyl sulfoxide; DP, declustering potential; EPI, enhanced product ion; GSH, glutathione; IDA, information-dependent acquisition; LC-MS/MS, liquid chromatography-tandem mass spectrometry; MRM, multiple-reaction monitoring; NAC, N-acetyl cysteine; NMR, nuclear magnetic resonance; Q-TOF, quadrupole/time-of-flight; PAPS, 3′-phosphoadenosine-5′-phosphosulfate; PCP，pentachlorophenol; PBS, phosphate-buffered saline; RLC，rat liver cytosol; SULTs, sulfotransferases.

## REFERENCES

(1) Yu, C. P., Shia, C. S., Lin, H. J., Hsieh, Y. W., Lin, S. P., Hou, Y. C. (2016) Analysis of the pharmacokinetics and metabolism of aloe-emodin following intravenous and oral administrations in rats. *Biomed. Chromatogr. 30*, 1641-1647.

(2) Lu, G. D., Shen, H. M., Chung, M. C., Ong, C. N. (2007) Critical role of oxidative stress and sustained JNK activation in aloe-emodin-mediated apoptotic cell death in human hepatoma cells. *Carcinogenesis. 28*, 1937-1945.

(3) Cárdenas, C., Quesada, A. R., Medina, M. A. (2006) Evaluation of the anti-angiogenic effect of aloe-emodin. *Cell. Mol. Life Sci. 63*, 3083-9.

(4) Krumbiegel, G., Schulz, H. U. (1993) Rhein and Aloe-Emodin Kinetics from Senna Laxatives in Man. *Pharmacology. 47*, 120-124.

(5) Agarwal, S. K., Singh, S. S., Verma, S., Kumar, S. (2000) Antifungal activity of anthraquinone derivatives from Rheum emodin. *J Ethnopharmacol. 72*, 43-46.

(6) Eshun, K., He, Q. (2004) Aloe vera: a valuable ingredient for the food, pharmaceutical and cosmetic industries–a review. *Crit Rev Food Sci Nutr. 44*, 91-96.

(7) Lee, H. Z., Wu, C. H., Chang, S. P. (2010) Release of nucleophosmin from the nucleus: Involvement in aloe-emodin-induced human lung non small carcinoma cell apoptosis. *Int. J. Cancer. 113*, 971-976.

(8) Kuo, P. L., Lin, T. C., Lin, C. C. (2002) The antiproliferative activity of aloe-emodin is through p53-dependent and p21-dependent apoptotic pathway in human hepatoma cell lines. *Life Sci. 71*, 1879-1892.

(9) Shieh, D. E., Chen, Y. Y., Yen, M. H. Chiang, L. C., Lin, C. C. (2004) Emodin-induced apoptosis through p53-dependent pathway in human hepatoma cells. *Life Sci. 74*, 2279-2290.

(10) Pecere, T., Gazzola, M. V., Mucignat, C., Parolin, C., Vecchia, F. D., Cavaggioni, A., Basso, G., Diaspro, A., Salvato, B., Carli, M., Palu, G. (2000) Aloe-emodin is a new type of anticancer agent with selective activity against neuroectodermal tumors. *Cancer Res. 60*, 2800-2804.

(11) Pecere, T., Sarinella, F., Salata, C., Gatto, B., Bet, A., Dalla Vecchia, F., Diaspro, A., Carli, M., Palumbo, M., Palu, G. (2003) Involvement of p53 in specific

anti-neuroectodermal tumor activity of aloe-emodin. *Int J Cancer. 106*, 836-847.

(12) Swanbeck, G. (1966) Interaction between deoxyribonucleic acid and some anthracene and anthraquinone derivatives. *Biochim. Biophys. Acta. 123*, 630-633.

(13) Al-Otaibi, J. S., Spittle, P. T., Gogary, T. M. E. (2017) Interaction of anthraquinone anti-cancer drugs with DNA: Experimental and computational quantum chemical study. *J Mol Struct. 1127*, 751-760.

(14) Westendorf, J., Marquardt, H., Poginsky, B., Dominiak, M., Schmidt, J., Marquardt, H. (1990) Genotoxicity of naturally occurring hydroxyanthraquinones. *Mutat Res. 240*, 1-12.

(15) Panigrahi, G. K., Verma, N., Singh, N., Asthana, S., Gupta, S. K., Tripathi, A., Das, M. (2018) Interaction of anthraquinones of Cassia occidentalisseeds with DNA and Glutathione. *Toxicol Rep. 5*, 164-172.

(16) Weinshilboum, R. M. (1986) Phenol sulfotransferase in humans: properties, regulation, and function. *Fed Proc. 45*, 2223-2228.

(17) Coughtrie, M. W. H., Sharp, S., Maxwell, K., Innes, N. P. (1998) Biology and function of the reversible sulfation pathway catalysed by human sulfotransferases and sulfatases. *Chem Biol Interac. 109*, 3-27.

(18) Falany, C. N. (1991) Molecular enzymology of human liver cytosolic sulfotransferases. *Trends Pharmacol Sci. 12*, 255-9.

(19) Coughtrie, M. W. (1996) Sulphation catalysed by the human cytosolic sulphotransferases -- Chemical defence or moleculartерrorism? *Hum Exp Toxicol. 15*, 547-555.

(20) Frederick, C. K. P. D. (1994). Conjugation-Deconjugation Reactions in Drug Metabolism and Toxicity. *Springer Berlin Heidelberg. 46*, 2434-2445.

(21) Diao, X., Pang, X., Xie, C., Guo, Z., Zhong, D., Chen, X. (2014) Bioactivation of 3-n-butylphthalide via sulfation of its major metabolite 3-hydroxy-NBP: mediated mainly by sulfotransferase 1A1. *Drug Metab Dispos. 42*, 774-781.

(22) Ishii, Y., Okamura, T., Inoue, T., Fukuhara, K., Umemura, T., Nishikawa, A. (2010) Chemical Structure Determination of DNA Bases Modified by Active Metabolites of Lucidin-3-O-primeveroside. *Chem Res Toxicol. 23*,134-141.

(23) Wang, X., Sun, Y., Zou, L. Z., Li, H., Zhao, Y. F., Li, R. H., Peng, Y., Zheng, J. Chemical Reactivity of Aloe-Emodin and Its Hydroxylation Metabolites to Thiols. *Chem Res Toxicol.* doi: 10.1021/acs.chemrestox.8b00248.

(24) Ma, J. Y., Zhou, X., Fu, J. (2014) Metabolite profiling analysis of FR429, an ellagitannin purified from Polygonum capitatum, in rat and human liver microsomes, cytosol and rat primary hepatocytes in vitro. *Chem Biol Interact. 220*, 33-40.

(25) Shao, J. W., Xiang, L. P., Jiang, M. H, Yang, X., Wang, W. F. (2014) Aloe emodin quaternary ammonium salt as well as preparation and application thereof. *CN 103896790 A*.

(26) Meerman, J. H., Beland, F. A., Ketterer, B., Srai, S. K., Bruins, A. P., Mulder, G. J. (1982) Identification of glutathione conjugates formed from N-hydroxy-2-acetylaminofluorene in the rat. *Chem Biol Interact. 39*, 149-168.

(27) Jeurissen, S. M. F., Punt, A., Delatour, T., Rietjens, I. M. (2008) Basil extract inhibits the sulfotransferase mediated formation of DNA adducts of the procarcinogen 1′-hydroxyestragole by rat and human liver S9 homogenates and in HepG2 human hepatoma cells. *Food Chem Toxicol*. *46*, 2296-2302.

(28) Yan, Z., Maher, N., Torres, R., Huebert, N. (2007) Use of a trapping agent for simultaneous capturing and high-throughput screening of both “soft” and “hard” reactive metabolites. *Anal. Chem. 79*, 4206-4214.

(29) Poon, G. K., Chen, Q., Teffera, Y., et al. (2001) Bioactivation of diclofenac via benzoquinone imine intermediates-identification of urinary mercapturic acid derivatives in rats and humans. *Drug Metab Dispos. 29*, 1608-1613.

(30) Clapp, J. J., Young, L. (1970) Formation of mercapturic acids in rats after the administration of aralkyl esters. *Biochem J. 118*, 765-771.

**Table 1**. Mass spectrometric profiling data of AE-GSH/NAC conjugates obtained from LC-Q-TOF MS analysis.

**Figure Legends**

**Figure 1.** Characterization of AE-GSH conjugate. Chromatograms of extracted ion (*m*/*z* 560/253) obtained from LC-Q-Trap MS analysis of rat liver cytosol incubations fortified with AE and GSH in the absence (A) or presence (B) of PAPS. C: Chromatograms of extracted ion obtained from LC-Q-Trap MS analysis of synthetic AE-GSH conjugate. D: MS/MS spectrum of AE-GSH conjugate produced in cytosol incubations. E: MS/MS spectrum of synthetic AE-GSH conjugate.

**Figure 2.** Characterization of AE-NAC conjugate. Chromatograms of extracted ion (*m*/*z* 416/253) obtained from LC-Q-Trap MS analysis of rat liver cytosol incubations supplemented with AE and NAC in the absence (A) or presence (B) of PAPS. C: Chromatograms of extracted ion obtained from LC-Q-Trap MS analysis of synthetic AE-NAC conjugate. D: MS/MS spectrum of AE-NAC conjugate produced in cytosol incubations. E: MS/MS spectrum of synthetic AE-NAC conjugate.

**Figure 3.** Characterization of compound **1** (AE-Br). Chromatograms of extracted ions (*m/z* 333/254 and *m/z* 335/254) obtained from LC-MS/MS analysis of synthetic compound **1**.

**Figure 4.** Chemical structures (A) and $^{1}$H NMR chemical shifts (B) of AE-GSH/NAC conjugates.

**Figure 5.** Characterization of biliary AE-GSH and urinary AE-NAC conjugates.

Chromatograms of extracted ion (*m*/*z* 560/253 for AE-GSH) obtained from LC-Q-Trap MS analysis of bile of rats before (A) and after (B) treatment with AE. C: MS/MS spectrum of AE-GSH conjugate in bile samples of rats given AE. Chromatograms of extracted ion (*m*/*z* 416/253 for AE-NAC) obtained from LC-Q-Trap MS analysis of urine of rats before (D) and after (E) treatment with AE. F: MS/MS spectrum of AE-NAC conjugate in urine samples of rats given AE.

**Figure 6.** Effects of PCP on excretion of biliary AE-GSH conjugate (A) and urinary AE-NAC conjugate (B) in rats treated with AE. Rats pretreated with PCP (10 mg/kg, i.p.) or vehicle were given AE (200 mg/kg, i.p.). Bile samples and urine samples (n=3) were collected. The contents of AE-GSH/NAC conjugates were measured by LC-MS/MS. Data represent values from triplicate measurements. $^{**}p < 0.01$ (mean ± SD).

**Figure 7.** Effect of PCP (6.25 μM) on susceptibility of HepG2 cells to AE cytotoxicity. Each column represents the mean of triplicate samples. $^{*}p < 0.05$; $^{**}p < 0.01$ versus their respective incubations without pretreatment with PCP.

**Scheme Legends**

**Scheme 1**. Synthetic route of compound **1** (AE-Br).

**Scheme 2**. Proposed mechanisms of AE metabolic activation mediated by SULTs.

**Table 1**.

| compound | formula | [M+H]$^+$ | | error | | mSigma |
|---|---|---|---|---|---|---|
| | | calculated | detected | ppm | mDa | |
| AE-GSH | $C_{25}H_{25}N_3O_{10}S$ | 560.1333 | 560.1332 | 2.5 | 0.14 | 7.41 |
| AE-NAC | $C_{20}H_{17}NO_7S$ | 416.0798 | 416.0795 | 0.9 | 0.39 | 42.75 |

**Figure 1.**

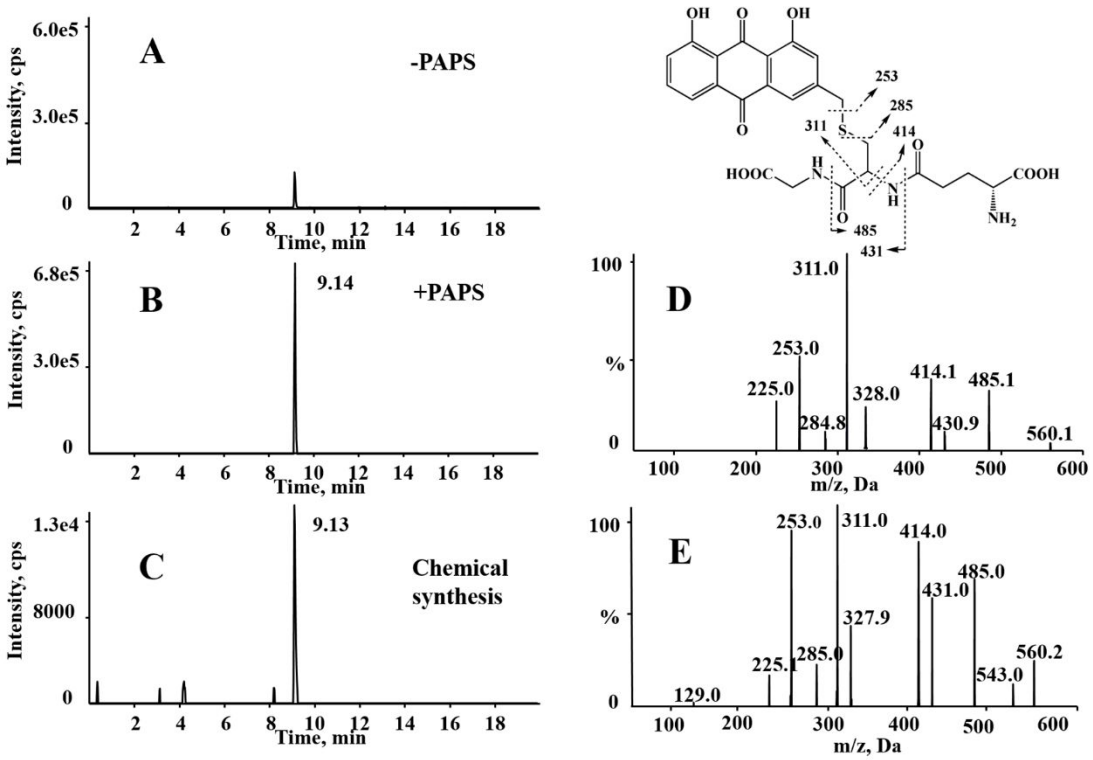
A
-PAPS
Intensity, cps
6.0e5
3.0e5
0
Time, min
B
+PAPS
9.14
6.8e5
C
Chemical synthesis
9.13
1.3e4
8000
D
311.0
253.0
225.0
284.8
328.0
414.1
430.9
485.1
560.1
m/z, Da
E
253.0
311.0
414.0
485.0
431.0
327.9
225.1
285.0
560.2
543.0
129.0
OH
HOOC
COOH
NH2
253
285
311
414
485
431

**Figure 2.**

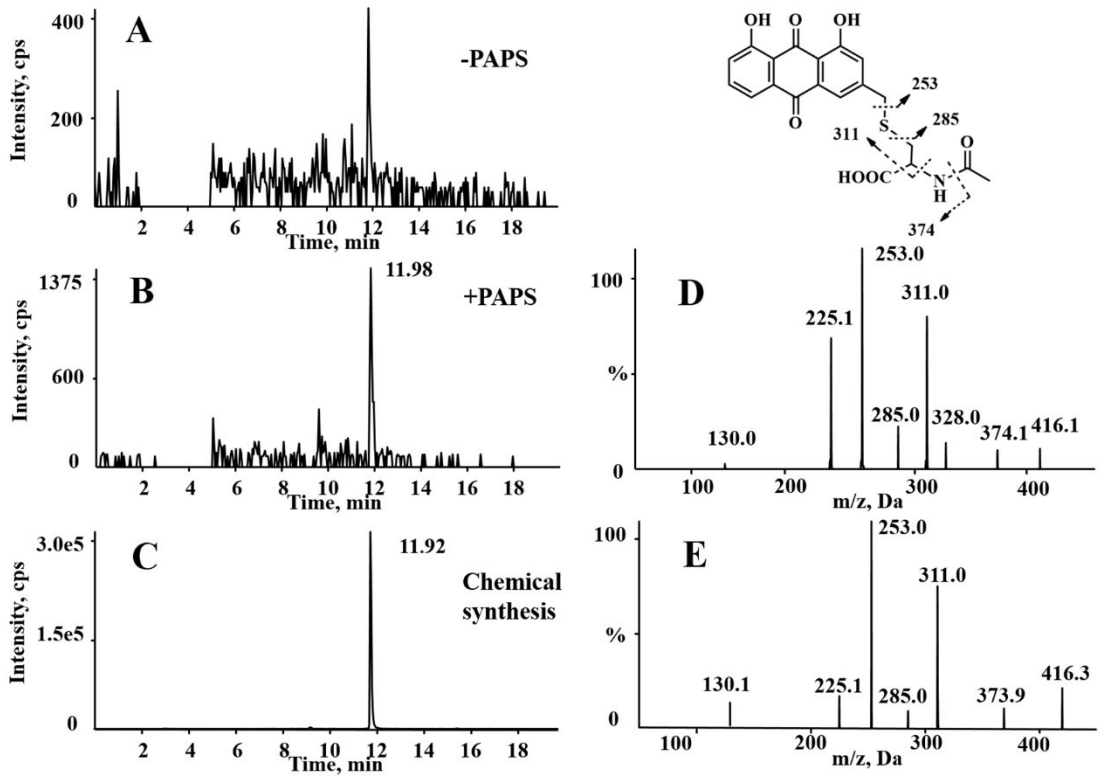
A
-PAPS
Intensity, cps
400
200
0
2 4 6 8 10 12 14 16 18
Time, min
B
+PAPS
11.98
1375
600
C
Chemical synthesis
11.92
3.0e5
1.5e5
OH O OH
O
253
285
311
S
HOOC
N
H
O
374
D
253.0
311.0
225.1
285.0
328.0
374.1
416.1
130.0
100
%
m/z, Da
E
253.0
311.0
130.1
225.1
285.0
373.9
416.3

**Figure 3.**

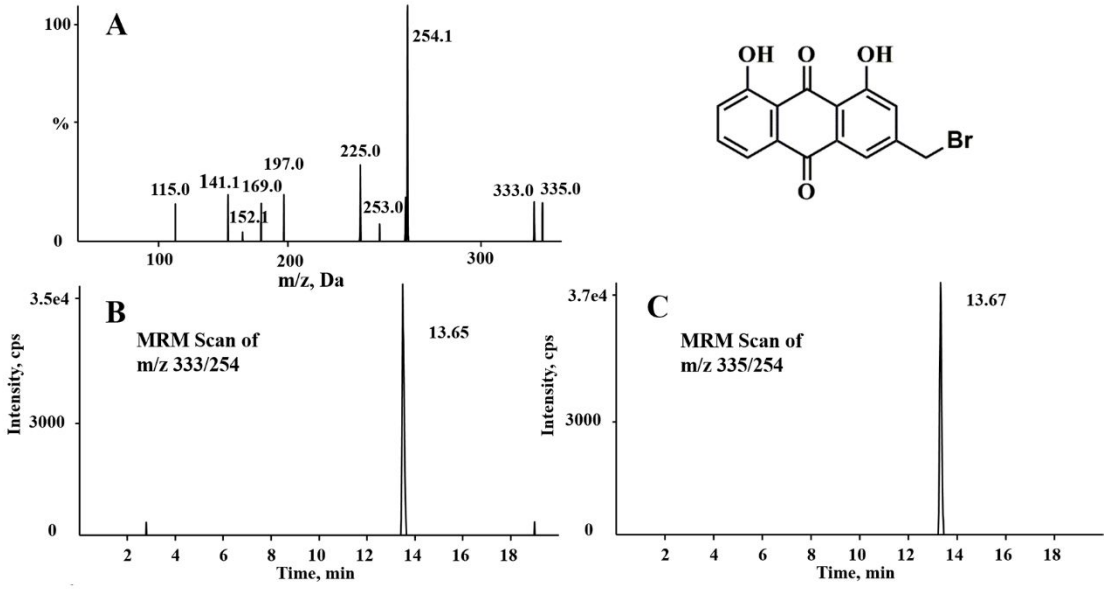
A
100
%
0
254.1
225.0
197.0
169.0
141.1
115.0
152.1
253.0
333.0
335.0
100
200
300
m/z, Da
OH
O
OH
Br
O
B
MRM Scan of
m/z 333/254
13.65
3.5e4
3000
0
Intensity, cps
2
4
6
8
10
12
14
16
18
Time, min
C
MRM Scan of
m/z 335/254
13.67
3.7e4
3000
0
Intensity, cps
2
4
6
8
10
12
14
16
18
Time, min

**Figure 4.**

**A**

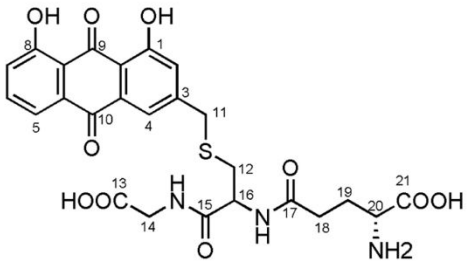

AE-GSH

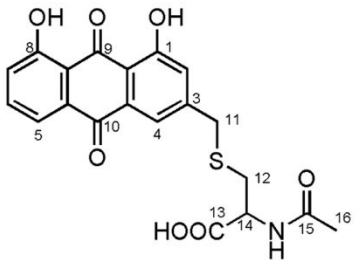

AE-NAC

**B**

| Proton | AE-GSH | AE-NAC |
|---|---|---|
| H-2 | 7.35 (1H, s) | 7.33 (1H,s) |
| H-4 | 7.68 (1H, s) | 7.71 (1H, s) |
| H-5 | 7.71 (1H, d , *J*= 7.4 Hz ) | 7.73 (1H, d, *J*= 7.5 Hz) |
| H-6 | 7.80 (1H, dd, *J*= 7.9,7.9 Hz) | 7.83 (1H, dd, *J*= 7.6,8.0 Hz) |
| H-7 | 7.36 (1H, d, *J*= 8.3 Hz) | 7.40 (1H, d, *J*= 8.3 Hz) |
| H-11 | 3.72 (2H, m) | 3.90 (2H, s) |
| H-12 | 2.61 (1H, dd, *J*= 4.1, 13.3 Hz)<br>2.83 (1H, dd, *J*= 4.5, 13.7 Hz) | 2.69 (1H, dd, *J*= 4.8,13.6 Hz)<br>2.83 (1H, dd, *J*= 8.5,13.6 Hz ) |
| H-14 | 2.54 (2H, s) | 4.39 (1H, m) |
| N-H | - | 8.28 (1H, d, *J*= 7.9 Hz) |
| H-16 | 4.52 (1H, dd, *J*= 8.8, 13.4 Hz) | 1.86 (3H, s) |
| N1'-H | 8.68 (1H, s) | - |
| N2'-H | 8.43 (1H, d, *J*= 8.5 Hz) | - |
| H-18 | 2.36 (2H, t, *J*= 6.5 Hz) | - |
| H-19 | 1.97 (2H, m) | - |
| H-20 | 3.42 (1H, s) | - |
| N3'-H | 3.87 (2H, d, *J*= 11.1 Hz ) | - |

**Figure 5.**

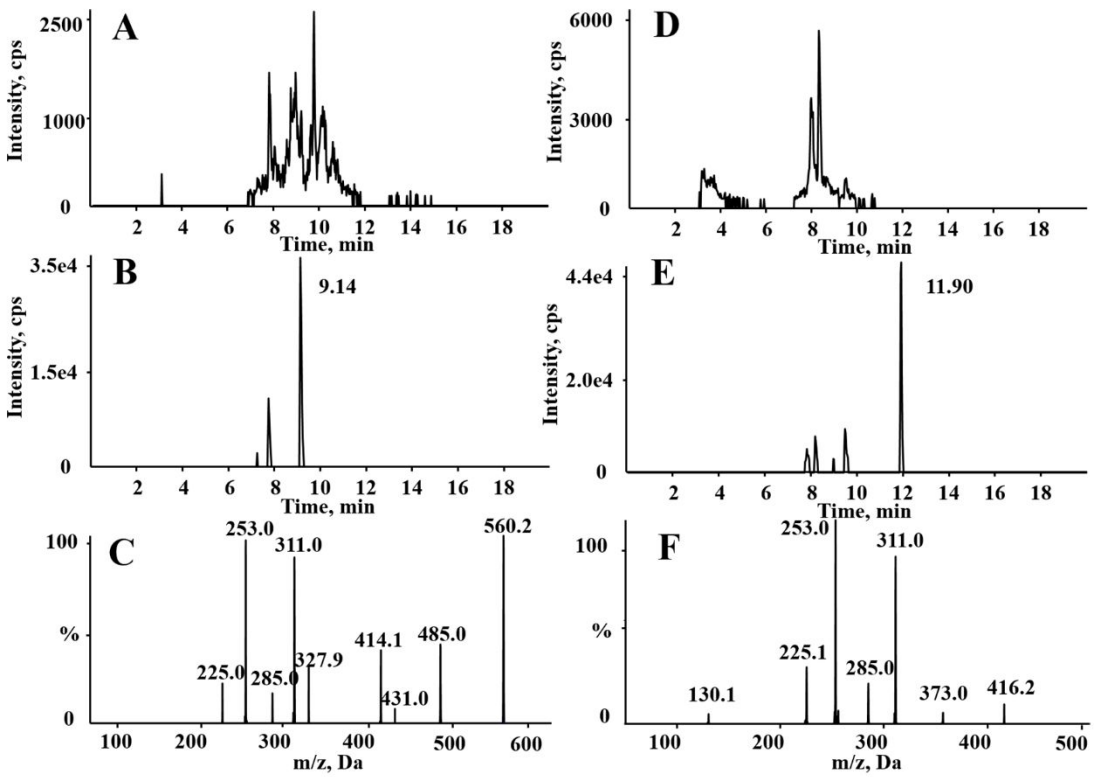
A
Intensity, cps
2500
1000
0
2 4 6 8 10 12 14 16 18
Time, min
D
Intensity, cps
6000
3000
0
2 4 6 8 10 12 14 16 18
Time, min
B
Intensity, cps
3.5e4
1.5e4
0
9.14
2 4 6 8 10 12 14 16 18
Time, min
E
Intensity, cps
4.4e4
2.0e4
0
11.90
2 4 6 8 10 12 14 16 18
Time, min
C
100
%
0
253.0
311.0
560.2
414.1
485.0
327.9
225.0
285.0
431.0
100 200 300 400 500 600
m/z, Da
F
100
%
0
253.0
311.0
225.1
285.0
130.1
373.0
416.2
100 200 300 400 500
m/z, Da

**Figure 6.**

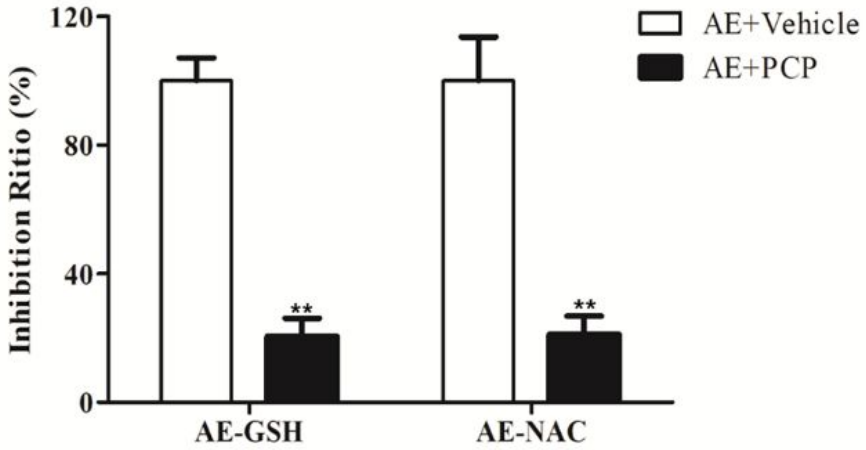

**Figure 7.**

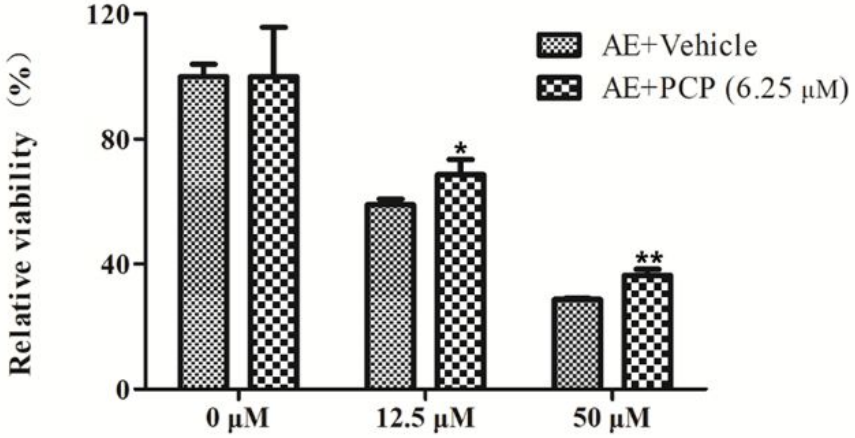
120
80
40
0
Relative viability (%)
AE+Vehicle
AE+PCP (6.25 μM)
*
**
0 μM
12.5 μM
50 μM

**Scheme 1**.

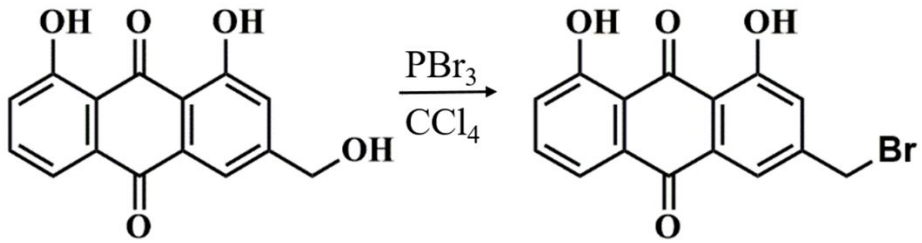

**Scheme 2**.

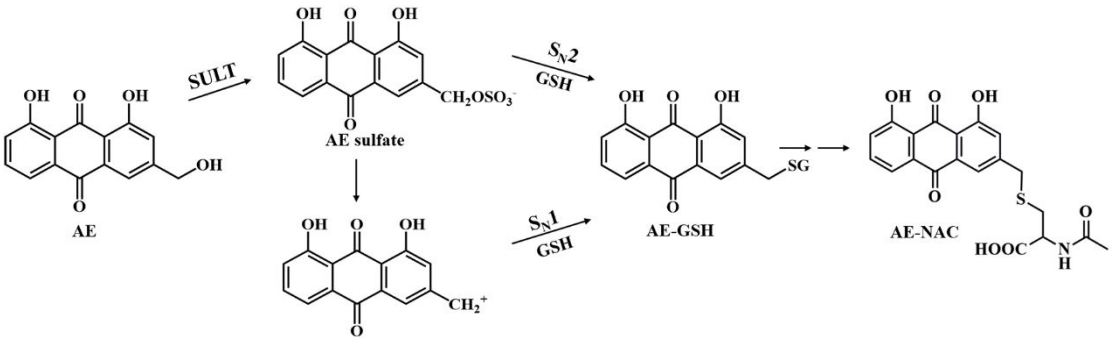
OH
O
OH
SULT
AE
OH
AE sulfate
CH2OSO3-
SN2
GSH
SG
AE-GSH
SN1
GSH
CH2+
S
HOOC
N
H
AE-NAC